NASA DEVELOP National Program
Massachusetts – Boston

Summer 2024

Alaska Ecological Conservation II

Using NASA Earth Observations to Identify Recent Changes in Vegetation Phenology and its Impacts on Caribou Calving and Migration

DEVELOP Technical Report
August 9th, 2024

Jackie Encinas (Project Lead)
Levi Mitchell (Project Lead)
Gareth Miller
Peter Vailakis

Advisors:
Dr. Mark Friedl, Boston University (Science Advisor)
Seamore Zhu, Boston University (Science Advisor)

Previous Contributors:
Christian Sarro
Levi Mitchell
Mahnoor Naeem
Ben Silver

Lead:
Madison Arndt (Massachusetts – Boston)

1. Abstract

Caribou are known for their long-distance migrations from wintering grounds to specified calving zones. Notably, the Western Arctic Herd (WAH) is the largest caribou herd in Northwestern Alaska that exhibits this behavior. These calving zones are highly predictable, and research suggests that calving and the availability of high-quality vegetation are correlated. We partnered with the U.S. National Park Service in Northwestern Alaska to use Terra and Aqua Moderate Resolution Imaging Spectroradiometer (MODIS) and Harmonized Landsat and Sentinel-2 (HLS) imagery to derive Normalized Difference Vegetated Index (NDVI) values and assess vegetation phenology in calving zones from 2000 – 2024. Our partners seek to understand if observed changes in caribou migration patterns and calving events correlate with shifts in the availability of nutrient-rich vegetation. Our results showed spatial variations of highly vegetated zones and annual shifts in the timing and length of growing seasons. While limitations existed in the MODIS and HLS datasets, we demonstrated feasibility using National Aeronautics and Space Administration (NASA) Earth observations for NDVI analysis over the study region. Using location data, our results may further research into caribou calving behaviors.

Key Terms

NDVI, NBAR, MODIS, HLS, Western Arctic Herd (WAH), Caribou, Calving, Alaska

2. Introduction

2.1 Background Information and Scientific Basis

Caribou (*Rangifer tarandus*) are one of the most abundant and ecologically significant terrestrial species in the Arctic. They play a crucial role in the nutrient transfer among tundra, boreal forests, and aquatic ecosystems, which support vegetation structures and Arctic food webs (Joly et al., 2021a). Additionally, caribou exhibit remarkable behavioral and physiological adaptability, enabling them to thrive in diverse environments from wet temperate forests to the polar deserts of the high Arctic (Joly et al., 2021a). Their ability to persist through a millennium of dramatic climatic changes may be a deciding factor in their ability to survive in the current era of climate change.

A hallmark of caribou's persistence is defined by their long-distance terrestrial migrations to specified calving areas. Caribou exhibit strong fidelity to distinct calving zones and use memory-based migratory routes (Nicholson et al., 2016). The Western Arctic Herd (WAH) relies on annual calving regions used by over 80% of the herd (Cameron et al., 2020). Migratory behaviors are crucial for understanding ecosystem ecology, which is dependent on habitat quality, climate change, predator presence, and human disturbances (Joly et al., 2021b). Interannual variations in weather and resource availability cause caribou to migrate and optimize calving to coincide with the seasonal peak of food availability (Post et al., 2003).

Natural and anthropogenic challenges are key contributors to the WAH's population decline and shifts in calving times (Mallory & Boyce, 2018). Wildlife biologists seek to understand population drivers; however, fieldwork in the Arctic makes tracking these changes in caribou difficult. Remote sensing data applications have long been used to non-invasively monitor animal species, climate phenomena, and vegetation quality. The Normalized Difference Vegetation Index (NDVI) is a remote sensing technique that estimates vegetation phenology by measuring the timing and magnitude of foliar greenness (Swanson, 2021). Pettorelli et al. (2005) found that NDVI provides an accurate representation of the plant phenology of an area and can be used to understand patterns of migration or habitation based on the relationship between an organism's biotic needs and the ability of a region to provide those needs. Previous research has successfully analyzed vegetation phenology by implementing NDVI indices through Terra and Aqua Moderate Resolution Imaging

Spectroradiometer (MODIS), Landsat, and Sentinel-2 imagery datasets (Karlson et al., 2021; Swanson, 2017; Swanson, 2021). Swanson's (2017 & 2021) tracked snow cover, green-up, peak green-up, and senescence in Alaska and used cameras to ground-truth satellite observations. Their results demonstrated the utility of NDVI indices to accurately track long-term greenness trends in the Arctic (Swanson, 2017; Swanson, 2021).

Our study follows the Spring 2024 NASA DEVELOP Alaska Ecological Conservation I project in collaboration with the National Park Service, which aimed to evaluate the feasibility of remote sensing techniques to monitor river ice phenology and its effect on caribou migration. Using Sentinel-1 synthetic aperture radar (SAR) imagery, the previous team identified physical state changes of Alaskan rivers during the fall season, from water to partial ice to completely frozen over. SAR imagery proved highly effective at distinguishing phase changes in river ice due to its ability to penetrate through clouds. Furthermore, optical imagery using Sentinel 2A/B, Landsat 8, and Landsat 9 improved temporal resolution and verified river conditions on cloudless images (Sarro et al., 2024). The team's analysis suggested unpredictable freezing times disrupted or deflected caribou migration.

2.2 Study Area and Study Period

Joly et al. (2021b) defined two key calving regions for WAH. Site A represents High-Density Calving (7,500km2), and Site B represents Low-Density Calving (54,500km2) (Figure 1). The calving zones overlap with the National Petroleum Reserve of Alaska (NPRA), which is managed by the U.S. Bureau of Land Management for oil and gas development and wildlife protection. To the south of Site A are park units of the U.S. National Park Service's Arctic Inventory and Monitoring Network (AIMN): Bering Land Bridge National Preserve, Cape Krusenstern National Monument, Gates of the Arctic National Park and Preserve, Kobuk Valley National Park, and Noatak National Preserve (Figure 2).

To analyze vegetation phenology and its correlation to caribou calving, our study concentrated on observations covering the WAH's peak calving period from May 25th - June 15th. We collected data using Aqua and Terra MODIS sensors from May 1st - July 5th over a 24-year period (2000-2024). Additionally, we utilized Harmonized Landsat 8 OLI, Landsat 9 OLI-2, and Sentinel-2 MSI sensors (HLS) to gather data from June - August over a 7-year span (2016-2023).

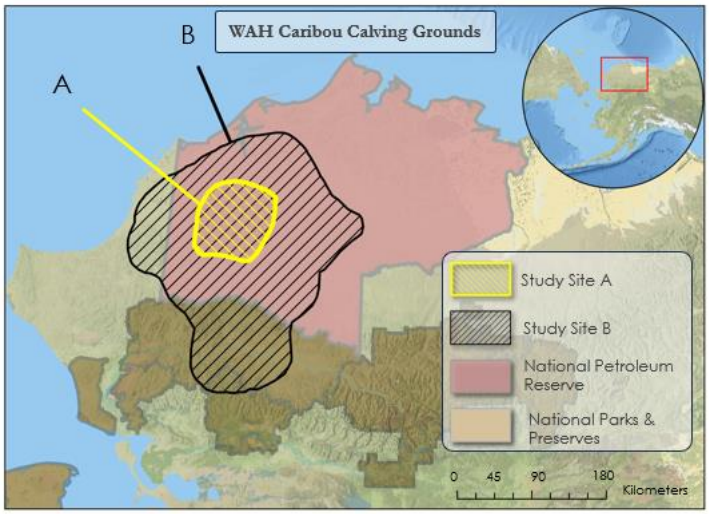

Figure 1. Study area map showing High-Density Calving Areas (Site A) and Low-Density Calving Areas (Site B) in relation to US National Park and National Petroleum Reserve boundaries.

2.3 Project Partners and Objectives

This project partnered with the U.S. National Park Service, Gates of the Arctic National Park and Preserve to investigate changes in vegetation phenology patterns within key WAH calving areas. Gates of the Arctic is part of the Arctic Inventory and Monitoring Network (Figure 2). In recent years, the timing of caribou migration has shifted, and our project partners aimed to determine if these shifts are due to changes in vegetation phenology. They were also interested in knowing the extent of high-quality calving grounds in proximity to the NPRA boundary. This project used remotely sensed data from the Aqua and Terra MODIS, Sentinel-2 MSI, and Landsat 8 and 9 OLI satellite products to quantify seasonal changes. We aimed to identify and analyze green-up, seasonal vegetation, and cycle peaks in calving zones, utilizing NDVI through time-series plots and maps.

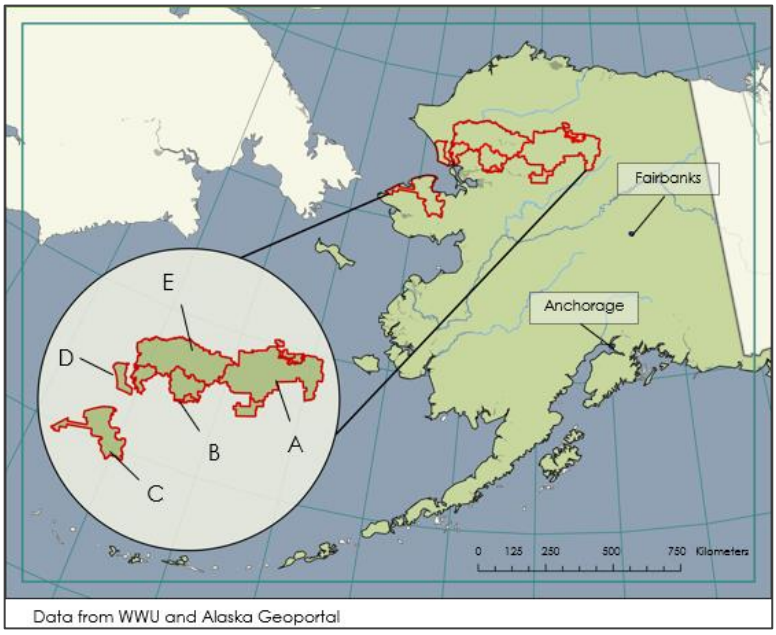

Figure 2. Map of the US National Park Service Arctic Inventory and Monitoring Network. A) Gates of the Arctic National Park and Preserve. B) Kobuk Valley National Park. C) Bering Land Bridge National Preserve. D) Cape Krusentern National Monument. E) Noatak National Preserve.

3. Methodology

3.1 Data Acquisition

We obtained remotely sensed data from the Terra and Aqua MODIS sensors, filtered between the dates May 1 – July 5, 2000 – 2024 from the MODIS MCD43A4 Version 6.1 Nadir Bidirectional Reflectance Distribution Function-Adjusted Reflectance (NBAR) dataset. This product produces daily 500-meter spatial resolution imagery, based on a 16-day retrieval period with image dates occurring on the 9th day. The NBAR algorithm chose the best representative pixel over the 16-day period and further pre-processed imagery with atmospheric corrections, cloud masking, bidirectional reflectance distribution function (BRDF) corrections, and temporal smoothing. We acquired this imagery through Google Earth Engine, Web API v0.1.413 (GEE), a code-based spatial analysis software that allows for easy and efficient image analysis at regional and continental scales.

Using the NASA EarthData web site, we obtained HLS imagery from the Sentinel-2A/B Multispectral Imaging (MSI) sensor, along with data from the Landsat 8 and Landsat 9 Operational Land Imager (OLI and OLI-2) sensors, covering the years 2016 to 2023. Sentinel-2 MSI and Landsat 8 and 9 OLI/OLI-2 data

undergo pre-processing steps, including atmospheric corrections, cloud masking, geometric resampling, geographic registration, BRDF normalization, and bandpass adjustments. These datasets are then integrated to produce the Harmonized Landsat and Sentinel-2 (HLS) product, which provides consistent 30-meter spatial resolution observations at a 2–3-day temporal revisit resolution.

Table 1.
Remote sensing data acquired from Google Earth Engine.

Sensor	Processing Level	Spatial Resolution	Data Provider	GEE Image Collection ID	Product
Terra MODIS	Level 3	500 meters	NASA LP DAAC	MODIS/061/MCD43A4	MODIS NBAR
Aqua MODIS	Level 3	500 meters	NASA LP DAAC	MODIS/061/MCD43A4	MODIS NBAR
Landsat Global Inland Water	Level 4 (derived product)	30 meters	NASA LP DAAC	GLCF/GLS_WATER	Water mask

Table 2.
Remotely sensed data acquired from NASA EarthData Search.

Sensor	Processing Level	Spatial Resolution	Data Provider	Product
Sentinel 2A/B MSI	Level 1-C	30 meters	European Union/ESA/Copernicus	HLSS30 v015
Landsat 8 OLI	Level 1	30 meters	NASA LP DAAC	HLSL30 v002
Landsat 9 OLI-2	Level 1	30 meters	NASA LP DAAC	HLSL30 v002

3.2 Data Processing

We processed our NBAR MODIS dataset in GEE. Our script included a function to derive NDVI as a new band using the NDVI equation (Equation 1; Tucker, 1979). We added NDVI bands to each image in the dataset and removed negative NDVI values by applying a 0 NDVI minimum pixel limit and a water mask rendered from the Landsat Global Inland Water dataset. We filtered the bounds of the dataset to study Site B annually from May – July 5, 2000 – 2024.

$$NBAR\ MODIS\ NDVI\ = \frac{NIR - Red}{NIR + Red} = \frac{Band\ 2\ (841 - 876) - Band\ 1\ (620 - 670)}{Band\ 2\ + Band\ 1}$$

(Equation 1)

We used HLS imagery in the Multi-Source Land Surface Phenology (MSLSP) algorithm produced by Friedl (2021) to derive Day of Year (DOY) surface phenology metrics for the years 2016 – 2023. The phenology metrics generated from the MSLSP product included separate bands for the annual DOY value (1-365) per pixel for the key phenology stages listed in Table 4. The MSLSP product also provided numeric values for the NDVI amplitude, maximum, and quality assurance measurements during the vegetation cycle. We extracted area-level zonal statistics of phenology metrics per-pixel DOY values by applying mean and median reducers in GEE. Next, we converted DOY values to their corresponding calendar date.

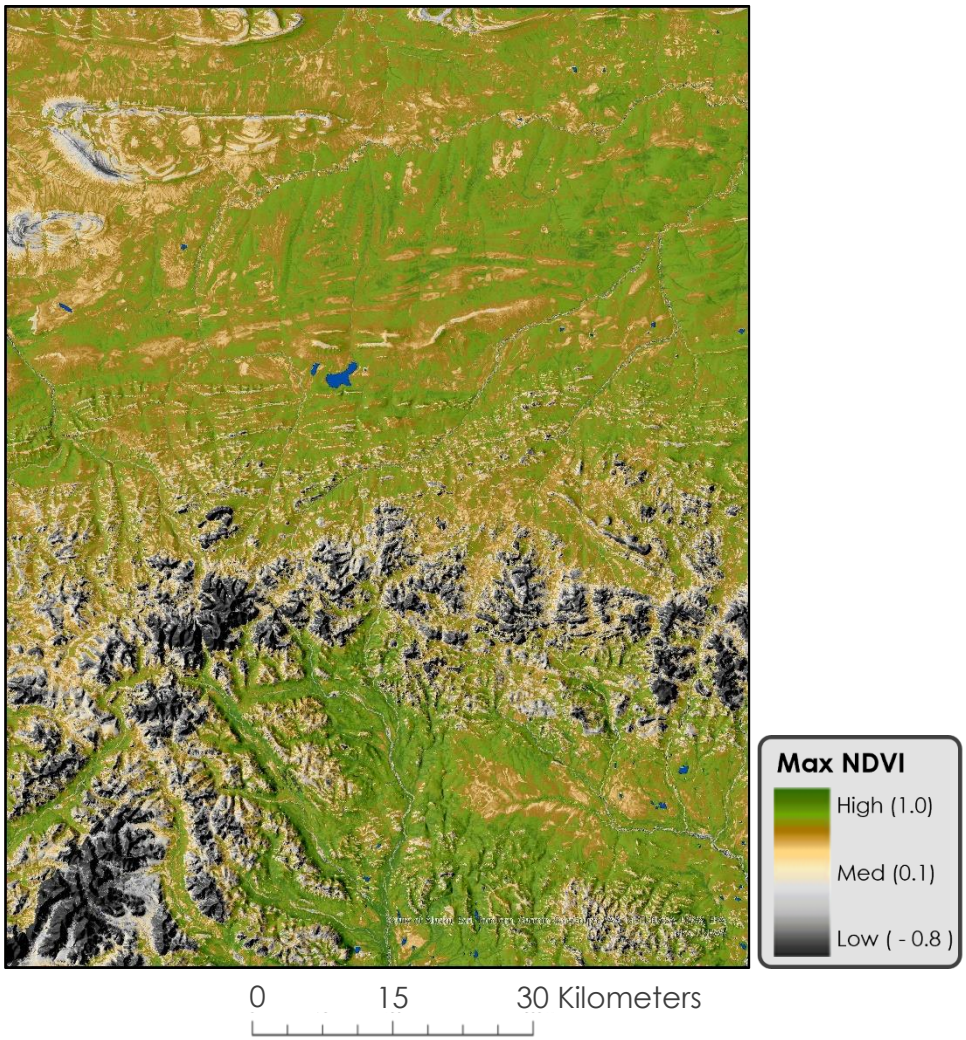

Figure 3. 2016 maximum NDVI taken for part of Study Area B (from HLS data).

Table 4
Vegetation phenology generated from MSLSP product.

Band #	Layer Name	Short Title	Phenological Parameter Description
1	Onset Greenness Increase Date	OGI	Date of 15% greenness increase relative to minimum NDVI
2	50% Greenness Increase Date	50PCGI	Date of 50% greenness increase relative to minimum NDVI
3	Onset Greenness Maximum Date	OGMx	Date of 90% greenness increase relative to minimum NDVI
4	Peak Greenness Date	Peak	Date of cycle peak
5	Onset Greenness Decrease Date	OGD	Date of 10% greenness decrease relative to maximum NDVI
6	50% for Greenness Decrease Date	50PCGD	Date of 50% greenness decrease relative to maximum NDVI
7	Onset Greenness Minimum Date	OGMn	Date of 85% greenness decrease relative to maximum NDVI
8	NDVI Max	NDVImax	Maximum NDVI during vegetation cycle

9	NDVI Amplitude	NDVIamp	NDVI amplitude during vegetation cycle
10	Green-up QA	gupQA	Quality assurance for green-up segment

3.3 Data Analysis

For our analysis of the NBAR MODIS dataset, we used GEE to calculate the mean, median, maximum, and minimum NDVI values of each year of our study period from 2000 – 2024. We included a function in our script that plotted these four statistical values on time series plots for each year and a composite plot for all years to show changes in NDVI from May 1 – July 5. The NDVI statistical metrics for each year were exported as a CSV file and imported into Microsoft Excel v2406 for formatting and plotting. Additionally, we calculated the rate of change in NDVI, or Delta NDVI (ΔNDVI), during the green-up interval each year using a slope formula (Equation 2). Our start date (Date1) was the first date after the initial spike in NDVI, which is likely indicative of annual spring snowmelt. We consistently used June 25 as the end date (Date2) for our ΔNDVI analysis due to the end of calving and departure of caribou. The only exception to June 25 as the end date was in 2001, due to a data gap.

$$\Delta NDVI = \frac{NDVI_2 - NDVI_1}{Date_2 - Date_1}$$

(Equation 2)

After compiling the annual mean DOY for each phenology stage, we created time series plots for the MSLSP product in Excel. We created plots for each year and a composite plot of all years to show changes in the timing of phenology over the entire season. Each plot displayed the annual increase in NDVI scaled from 15-100%; however, our analysis did not include comparing differences in interannual NDVI peak values.

We produced time series maps for NBAR MODIS and MSLSP data in ArcGIS Pro version 3.3 to visualize spatial variations in vegetation over the study period. These plots utilized the NDVI features of each dataset respectively. For MSLSP, we visualized the median of peak NDVI values in Band 8 (Maximum NDVI), and for MODIS, we calculated median NDVI values. We used the same color ramp for all maps produced as part of the time series to ensure we could make a visual comparison. In addition to the time series maps, we created composite images for each data source representing the high values of NDVI for the study years.

We constructed the composite NDVI images of our study period from MODIS and HLS data. With MODIS NDVI data in GEE, we applied a reducer that calculated the median NDVI per year from 2000-2024. We merged all 25 images into a single image collection and applied a median reducer to create a median composite image. This median reducer function computed median NDVI pixel values between all images, creating our composite visualization. We created the 2016-2023 HLS composite image in ArcGIS Pro by applying a similar median compositing function, utilizing the raster calculator analysis tool. As a result, the finalized composite maps visualized areas with median (2000-2023 MODIS composite) and peak (2016-2023 HLS composite) NDVI growing season values, indicating spatial distributions of vegetation quality.

4. Results & Discussion

4.1 Analysis of Results

4.1.1 NBAR MODIS Time Series Plots

The time series plots from the NBAR MODIS dataset showed similar patterns each year. Maximum and median NDVI values increased rapidly from values near 0 to values ranging 0.4 – 0.6. Swanson (2021) observed a similar pattern, and the researchers concluded that this spike in NDVI is likely indicative of spring snowmelt rather than rapid vegetation growth. Following snowmelt, NDVI values continued to gradually increase through our last day of observations (July 5). It is important to note that data in 2001 was significantly limited due to a sensor error that resulted in a large data gap (Appendix D, Figure D2). We

represented these data gaps as missing data values in the corresponding time series plot, and the NDVI metrics for that year should be considered cautiously.

4.1.2 NBAR MODIS Time Series Maps

The NBAR MODIS time series maps depicted median pixel values of NDVI from May 1 - July 5 for each year in our study period (2000-2024). Interestingly, our maps consistently showed higher NDVI values south of the Brooks Range, whereas Site A is suggestive of moderate vegetation growth from year to year (Appendix B). Lower levels of predation or competition in Site A may be indicative of the WAH's fidelity toward this region over the southern end of the Brooks Range; however, future work could explore this further.

4.1.3 HLS Time Series Maps

We created time series maps (Appendix C) using 30-meter HLS imagery to display peak NDVI between 2016–2023. We used Band 8, Maximum NDVI During the Vegetation Cycle, of the MSLSP product to create our maps. These maps displayed the spatial distribution of NDVI peak values. We compared them year to year to facilitate observations regarding vegetation distribution changes. Within the HLS maps, we saw minimal variation across the vegetation color ramp, which we can attribute to our utilization of peak NDVI over other statistical measures such as median or mean NDVI.

4.1.4 MODIS Delta NDVI (ΔNDVI)

Our analysis of the NBAR MODIS ΔNDVI revealed the interannual variations in green-up length and NDVI rate of change in relation to our study period. For fifteen of the twenty-four years in our study, green-up started between May 17 and May 23 (Appendix A, Table A1). The average length of observed green-up prior to caribou departure was 33.8 days (about one month) (Appendix A, Table A1). During this time, the average daily ΔNDVI increase was 0.0054 per day, with the earliest observed start date occurring on May 12, 2019, and the latest green-up date occurring on June 4, 2000 (Appendix A, Table A1). The early 2000s typically had the latest snowmelt and shortest green-up duration (Table 5). However, our results indicated green-up durations lengthened each year until 2019. Afterwards, green-up durations were comparable with 2005-2008, demonstrated the variability that can occur across a multi-decadal time series.

Table 5.
Displaying trends of green-up duration intersecting with the calving period

4 Year Interval	Average Green-up Duration within Calving
2000-2004	26.60 days
2005-2008	31.00 days
2009-2012	36.50 days
2013-2016	39.25 days
2017-2020	38.50 days
2021-2024	32.75 days

Investigating individual years revealed the variability in green-up cycles during caribou calving. In 2019, 2018, and 2016, we observed the earliest snowmelt. These years were the only instances where green-up periods intersected calving for more than 40 days (Appendix A, Table A1). Meanwhile, the shortest vegetation availability window following snowmelt occurred in 2000, 2002, and 2008. The start of green-up occurred on either June 2 or 4 and resulted in 21-23 days of green-up before caribou departure (Appendix A, Table A1).

Overall, in the study years, the average ΔNDVI increase from initial green-up (day after snowmelt) to the end of calving (June 25th) was 0.1794 (Appendix A, Table A3). However, ΔNDVI varied within each season. During the first ten days, there was an average 0.0024 ΔNDVI increase per day (Appendix A, Table A3).

Furthermore, separating study years into halves revealed an average increase of 0.0039 ΔNDVI during the first half, while the second half was 0.0069 ΔNDVI (Appendix A, Table A4). Our results indicated that green-up cycles typically began with a gradual increase following snowmelt, with an increasing rate as the cycle progressed. These results could suggest that the highest density of nutrient-rich vegetation became available for caribou towards the latter half of calving. Lastly, it is important to note that NDVI is scaled from -1 to 1; since we observed median greenness within the study period average at a 0.1794 ΔNDVI increase per year, these small numeric increases indicated the rate at which green-up occurs.

4.1.5 NBAR MODIS and HLS Composite Images

The NBAR MODIS and HLS NDVI composite images (Appendix D) represent the median and peak NDVI values across the study period. The MODIS data values are the true median calculated between 24 images for each cell across 2000-2023. The HLS composite values represent the median of peak NDVI values between 8 images for each cell across 2016-2023. These two metrics helped define areas of high and low vegetation for the study area and provided a view of that spatial distribution. The two maps display noticeably different results, likely due to their different resolutions, NDVI metrics, and the time spans they covered.

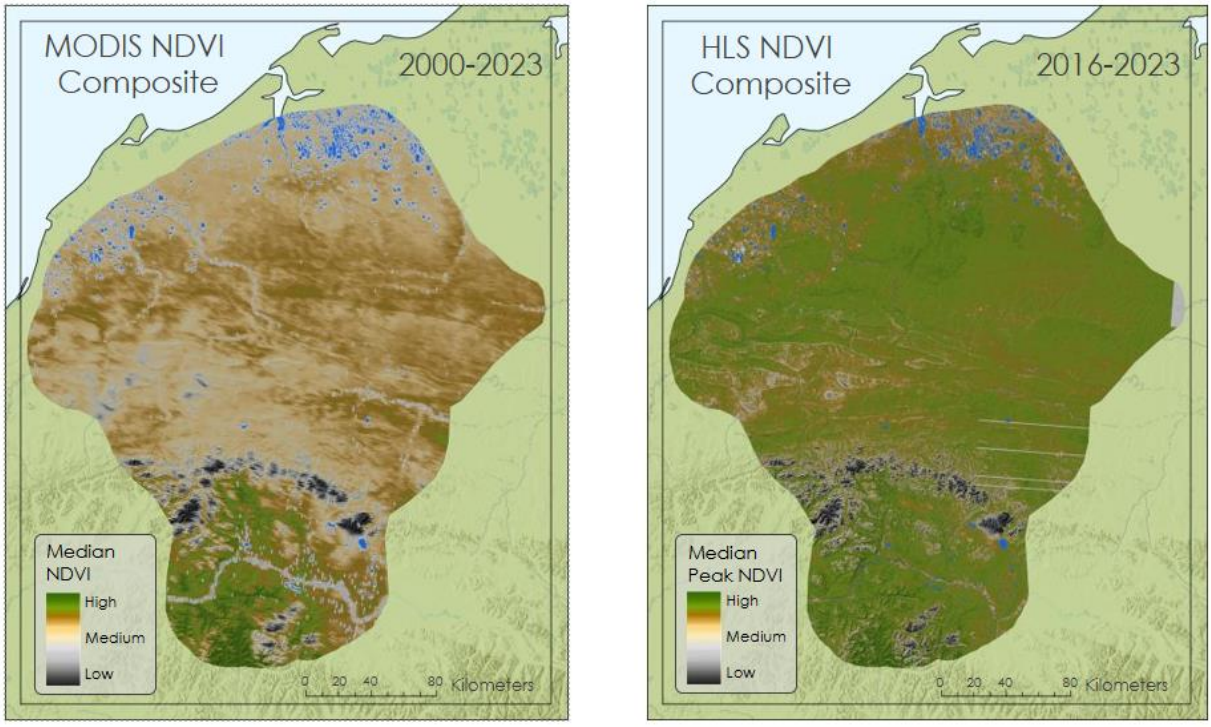

Figure 4. Composite Images of MODIS and HLS, Showing Median and Median Peak NDVI

4.1.6 HLS Phenology Curve

We constructed the HLS time series phenology curve using the MSLSP product. The plot showed the interannual shifting of phenology timing starting from the onset, midpoint increase, and cycle peak, followed by the onset of NDVI decrease, midpoint decrease, and greenness minimum. We scaled percent greenness from 0-1 per year, with 1 being the peak of the annual NDVI values from observations in a single season. The curve did not display changes in NDVI values each year; instead, we normalized the peaks to display the shift in timing of greening onset, midpoint increases and decreases, and peaks.

The HLS phenology curves (Figure 5) provided a larger context to Northwestern Alaska's vegetation phenology from May to September. Each year displayed the shifting key dates in the phenology cycle. The curve indicated a later start date than our MODIS analysis, this was due to the first data point representing a 15% greenness increase, while the MODIS analysis began the day after snowmelt. The years 2019 and 2020 had the earliest greenness onset on June 2nd and June 4th, while 2017 had the latest greenness minimum occurring on September 28th. Excluding 2019-2020, greenness onset occurred during June 10th-16th, while cycle peaks were in the range of July 23rd-31st.

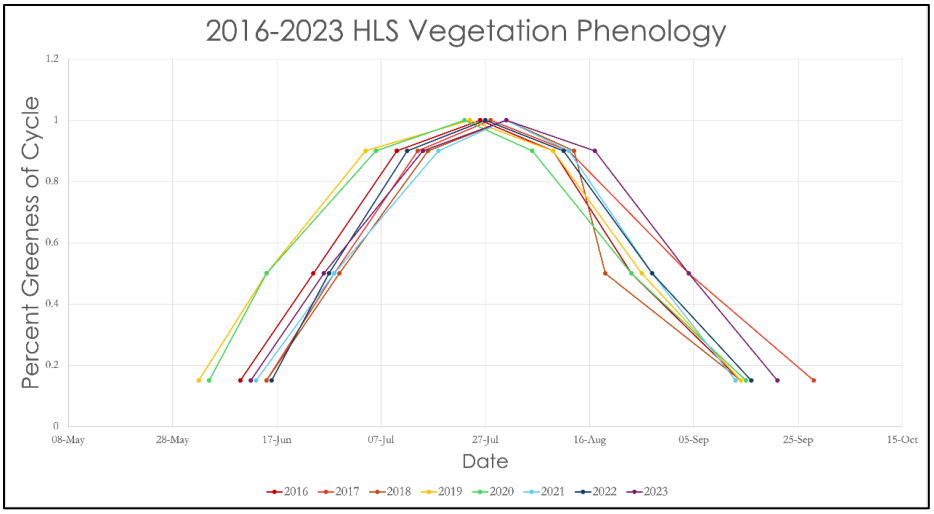

Figure 5. 2016-2023 HLS Vegetation Phenology Curve

4.2 Errors & Uncertainties

We encountered multiple errors and uncertainties that limited our results. We faced challenges in acquiring high-quality images from the NBAR MODIS dataset, as certain images contained significant cloud cover, which created data gaps and high levels of image error (A potential way around this is to use daily MODIS reflectance data instead of NBAR MODIS, however we did not have time to pursue this option). Additionally, the process we used to create a water mask for the NBAR MODIS dataset clipped 500-meter resolution water pixels to a 30-meter Landsat inland water dataset. The differences in spatial resolution meant that the water mask did not effectively clip all the water pixels. Because of this, we applied a surrounding buffer to further mask-out water pixels from our analysis. This process was imperfect and may have resulted in spottier imagery and affected our analysis.

Another source of uncertainty for the HLS time series maps was altering NDVI's representation scale from –1 to 1 to 0.1 to 1. For accurate visualization, we set 0.1 as the minimum NDVI value for a pixel to be considered vegetated; values below this threshold were colored black to indicate no vegetation. However, this adjustment may have misrepresented cells with NDVI values outside our defined threshold.

Furthermore, within the MODIS ΔNDVI analysis, there was a data gap due to a malfunction on the Terra MODIS sensor in 2001. We shortened the calving period during this year to the last available observation on June 19 and excluded it from calculations involving the study period. Additionally, the values of 0.0039 and 0.0069 are exceedingly small and fall within the +/- 0.01 MODIS NDVI uncertainty (Miura et al., 2000). As these daily change values are calculated from the change in two data points many days away from each other and not from two consecutive data points, it can still be said that ΔNDVI is greater in the second half of the year than in the first.

4.3 Feasibility & Partner Implementation

Despite limitations and uncertainties, our project demonstrated the effectiveness of using NBAR MODIS and HLS data to investigate vegetation phenology dynamics and monitor shifts in WAH caribou calving. We found that MODIS imagery was readily available over Northwestern Alaska. These MODIS images proved extremely valuable in deriving NDVI metrics across our study, despite their course resolution. While the MSLSP product produced a phenology curve for entire years, it was unsuitable for assessing vegetation green-up during the spring calving season (May 25 – June 15). The earliest date recorded in the HLS phenology product was June 2, approximately halfway into our study period, with the furthest date occurring in late September. Therefore, results from the MSLSP product may better assess summer and fall southbound caribou migrations as they correlate to shifts in vegetation green-up. Additionally, our science advisors at Boston University had to run the MSLSP algorithm on their servers, as it is not easily accessible to the public. Only those with Boston University credentials can run the script; therefore, our partner may not be able to run the algorithm without assistance from Boston University staff.

Our results can guide future research and conservation efforts within Gates of the Arctic National Park. Our partner may refine our analysis by improving the water mask and applying a snow filter to further remove low NDVI values. Additionally, our partner can apply aspects of our methods to summer and fall caribou migratory periods and may provide insight into how southbound migrations correlate with changes in vegetation. Our partner currently uses GIS and remote sensing techniques, which allows for integrating our methods into their workflow. They possess a GPS collar location dataset for caribou, which could facilitate future analysis of Alaskan caribou and NDVI.

5. Conclusions

Using NDVI time-series plots and maps, our study quantified Northwestern Alaska's dynamic interannual vegetation greenness phenology in relation to the WAH's calving period. Our partner can compare caribou behavior to determine relationships between vegetation phenology, caribou migration, and successful calving. Our results displayed the spatial distribution and timing of green-up relative to WAH calving behaviors. These results can inform our partner on the shifting vegetation metrics within the region.

Daily observations from NBAR MODIS provided a useful temporal resolution to observe the vegetation cycles within the study period from 2000-2024. ΔNDVI was a useful indicator for determining the rate of green-up and could provide insights into caribou migratory timings. Due to the high temporal resolution of MODIS observations, our analysis determined the rate of green-up for the first ten days following snowmelt, the first and second half of each year's calving period, and the calving period. Further analysis is required to determine if the summation of NDVI values can provide similar insights.

The MSLSP product provided high spatial-resolution imagery and Day-of-Year metrics displaying Northwestern Alaska's vegetation phenology from late May to late September. Using time-series maps and composite images, the 30-m pixel resolution provided useful data for displaying detailed spatial distributions of green-up patterns within the study area. The bands provided normalized DOY metrics relative to the peak growing season cycle date, allowing for comparable year-to-year timing estimates relative to DOY rather than NDVI values. However, the DOY metrics largely fell outside our study period of interest, extending beyond the duration of caribou calving. Greenness onset and midpoint increase dates were usually part-way through the study period, making high temporal resolution ΔNDVI analysis unfeasible. The HLS vegetation phenology product was therefore unable to observe any earlier trends. However, our partner can use these HLS phenology curves to investigate if the length of a season affects caribou southbound departures following calving. To better fit the HLS phenology curve within our study period, further research could extend the start date of the MSLSP algorithm by calculating DOY snowmelt pixel values prior to the 15% greenness increase.

Our results indicated that remote sensing was a useful method for determining the timing and quality of vegetation (in terms of greenness) during WAH caribou calving periods. We displayed the annual spatial

distribution of nutrient-dense vegetation and the timing of vegetative green-up. Our results may inform wildlife conservation efforts by identifying critical geographic locations crucial to caribou life cycles, including migration and calving.

6. Acknowledgements

The team would like to thank everyone who made this project possible:

- Dr. Kyle Joly (US NPS)
- Seamore Zhu (Boston University)
- Dr. Mark Friedl (Boston University)
- Madison Arndt (NASA DEVELOP Boston)

Special recognition goes to past contributors from the DEVELOP Spring 2024 Term:

- Christian Sarro (Project Lead)
- Levi Mitchell (Participant)
- Mahnoor Naeem (Participant)
- Ben Silver (Participant)

This material contains modified Copernicus Sentinel data (2016 - 2023), processed by ESA.

Any opinions, findings, and conclusions or recommendations expressed in this material are those of the author(s) and do not necessarily reflect the views of the National Aeronautics and Space Administration.

This material is based upon work supported by NASA through contract 80LARC23FA024.

7. Glossary

Earth observations – Satellites and sensors that collect information about the Earth's physical, chemical, and biological systems over space and time

HLS – Harmonized Landsat and Sentinel-2. Takes data from Landsat 8 OLI, Landsat 9 OLI-2, and Sentinel-2 A/B MSI satellites to generate a harmonized, analysis-ready surface reflectance data product

MODIS – Moderate Resolution Imaging Spectroradiometer

MSLSP – Multisource Land Surface Phenology product. The algorithm is used to derive day of year vegetation phenology metrics from Harmonized Landsat and Sentinel-2 data.

MSI – Multispectral Instrument. An instrument used on the Sentinel-2 A/B satellites to capture multispectral images at 20-meter resolution (visible, near infrared, shortwave-infrared).

NBAR – Nadir Bidirectional Reflectance Distribution Function-Adjusted Reflectance. An algorithm to model values (e.g. image pixels) as if they were collected from a nadir view.

NDVI – Normalized Difference Vegetation Index. A metric used to quantify the density, greenness, and health of vegetation.

OLI – Operational Land Imager. An instrument used on the Landsat 8 and Landsat 9 satellites to capture seasonal coverage of global landmass at a spatial resolution of 30-meters (visible, near infrared, shortwave-infrared).

WAH – Western Arctic Herd. Located in Alaska, the Western Arctic Herd is the largest caribou herd in the world.

8. References

Cameron, M., Joly, K., Breed, G. A., Mulder, C., & Kielland, K. (2020). Pronounced Fidelity and Selection for Average Conditions of Calving Area Suggestive of Spatial Memory in a Highly Migratory Ungulate. *Frontiers in Ecology and Evolution*, *8*. https://doi.org/10.3389/fevo.2020.564567

Friedl, M. (2021). *MuSLI Multi-Source Land Surface Phenology Yearly North America 30 m V011* [Data set]. NASA EOSDIS Land Processes Distributed Active Archive Center. https://doi.org/10.5067/Community/MuSLI/MSLSP30NA.011

Joly, K., Gunn, A., Côté, S. D., Panzacchi, M., Adamczewski, J., Suitor, M. J., & Gurarie, E. (2021a). Caribou and reindeer migrations in the changing Arctic. *Animal Migration*, *8*(1), 156–167. https://doi.org/10.1515/ami-2020-0110

Joly, K., Gurarie, E., Hansen, D. A., & Cameron, M. D. (2021b). Seasonal patterns of spatial fidelity and temporal consistency in the distribution and movements of a migratory ungulate. *Ecology and Evolution*, *11*(12), 8183–8200. https://doi.org/10.1002/ece3.7650

Mallory, C. D. & Boyce, M. S. (2018). Observed and predicted effects of climate change on Arctic caribou and reindeer. *Environmental Reviews*, *26*(1), 13–25. https://doi.org/10.1139/er-2017-0032

Masek, J., Ju, J., Roger, J., Skakun, S., Vermote, E., Claverie, M., Dungan, J., Yin, Z., Freitag, B., Justice, C. (2021). *HLS Operational Land Imager Surface Reflectance and TOA Brightness Daily Global 30m v2.0* [Data set]. NASA EOSDIS Land Processes Distributed Active Archive Center. Accessed 2024-07-10 from https://doi.org/10.5067/HLS/HLSL30.002

Masek, J., Ju, J., Roger, J., Skakun, S., Vermote, E., Claverie, M., Dungan, J., Yin, Z., Freitag, B., Justice, C. (2020). *HLS Sentinel-2 MSI Surface Reflectance Daily Global 30 m V1.5* [Data set]. NASA EOSDIS Land Processes Distributed Active Archive Center. Accessed 2024-07-10 from https://doi.org/10.5067/HLS/HLSS30.015

Miura, T., Huete, A. R., and Yoshioka, H. (2000). Evaluation of sensor calibration uncertainties on vegetation indices for MODIS. *IEEE Transactions on Geoscience and Remote Sensing*, *38*(3), 1399-1409. https://doi.org/10.1109/36.843034.

NASA EarthData. (2022, October 17). *Harmonized Landsat and Sentinel-2 (HLS).* ESDS Program. https://www.earthdata.nasa.gov/esds/harmonized-landsat-sentinel-2

NASA and USGS. (n.d.). *HLS Overview*. NASA EOSDIS Land Processes Distributed Active Archive Center. https://lpdaac.usgs.gov/data/get-started-data/collection-overview/missions/harmonized-landsat-sentinel-2-hls-overview/

Nicholson, K. L., Arthur, S. M., Horne, J. S., Garton, E. O., & Vecchio, P. A. D. (2016). Modeling Caribou Movements: Seasonal Ranges and Migration Routes of the Central Arctic Herd. *PLOS ONE*, *11*(4), e0150333. https://doi.org/10.1371/journal.pone.0150333

Pettorelli, N., Vik, J. O., Mysterud, A., Gaillard, J.-M., Tucker, C. J., & Stenseth, N. Chr. (2005). Using the satellite-derived NDVI to assess ecological responses to environmental change. *Trends in Ecology & Evolution*, *20*(9), 503–510. https://doi.org/10.1016/j.tree.2005.05.011

Post, E., Bøving, P., Pedersen, C., & MacArthur, M. (2003). Synchrony between Caribou calving and plant phenology in depredated and non-depleted populations. *Canadian Journal of Zoology-Revue Canadienne De Zoologie - CAN J ZOOL*, *81*, 1709–1714. https://doi.org/10.1139/z03-172

Sarro, C., Mitchell, L., Silver, B., Naeem, M. (2024). *Alaska Ecological Conservation: Using NASA Earth Observations to Identify Recent Changes in River Ice Phenology and Its Impacts on Caribou Migration* [Unpublished Manuscript]. NASA DEVELOP National Program, Massachusetts – Boston.

Schaaf, C. & Wang, Z. (2021). *MODIS/Terra+Aqua BRDF/Albedo Nadir BRDF Adjusted Ref Daily L3 Global - 500m V061* [Data set]. NASA EOSDIS Land Processes Distributed Active Archive Center. Accessed 2024-07-10 from https://doi.org/10.5067/MODIS/MCD43A4.061

Swanson, D. K. (2017). Trends in Greenness and Snow Cover in Alaska's Arctic National Parks, 2000–2016. *Remote Sensing, 9(6), Article 6*. https://doi.org/10.3390/rs9060514

Swanson, D. K. (2021). Start of the Green Season and Normalized Difference Vegetation Index in Alaska's National Parks. *Remote Sensing 13, no. 13*. 2554. https://doi.org/10.3390/rs13132554

Townshend, J. (2016). *Global Forest Cover Change (GFCC) Water Cover 2000 Global 30 m V001* [Data set]. NASA EOSDIS Land Processes Distributed Active Archive Center. Accessed 2024-07-10 from https://doi.org/10.5067/MEaSUREs/GFCC/GFCC30WC.001

Tucker, C.J. (1979). Red and photographic infrared linear combinations for monitoring vegetation. *Remote Sensing of Environment*, *8*(2), 127-150. https://doi.org/10.1016/0034-4257(79)90013-0.

9. Appendices

Appendix A: *MODIS Delta NDVI (*Δ NDVI)

Table A1

Summary of observed MODIS green-up within calving period, Δ*NDVI, and sum NDVI values for all study years.*

Summary				
Year	**Observed Green-Up**	**# of Days**	**ΔNDVI**	**ΣNDVI**
2000	June 4 – June 25	21	0.00761	10.5
2001[a.c.d.]	May 31 - June 19[d.]	19	0.00632	8.4
2002	May 19 - June 25	36	0.00414	17.5
2003[a.c.]	June 2 - June 25	23	0.00574	11.2
2004[a.]	May 22 - June 25	34	0.00688	17.8
2005[a.c.]	May 20 - June 25	36	0.00489	17.4
2006[a.c.]	May 25 - June 25	31	0.00668	14.9
2007	May 22 - June 25	34	0.00668	17.3
2008	June 2 - June 25	23	0.00661	12.3
2009[b.]	May 17 - June 25	39	0.00410	18.6
2010[a.]	May 19 - June 25	37	0.00541	18.1
2011	May 23 - June 25	33	0.00497	16.3
2012	May 19 - June 25	37	0.00519	18.4
2013	May 20 - June 25	36	0.00503	18.3
2014[c.]	May 17 - June 25	39	0.00431	17.5
2015	May 17 - June 25	39	0.00479	20.5
2016[a.c.]	May 13 - June 25	43	0.00516	21.4
2017	May 21 – June 25	35	0.00423	17.1
2018[a.c.]	May 15 - June 25	41	0.00456	18.8
2019[a.c.]	May 12 - June 25	44	0.00664	22.7
2020[a.b.]	May 22 - June 25	34	0.00632	18.6
2021[a.]	May 24 - June 24	32	0.00491	15.6
2022[a.c.]	May 28 - June 25	28	0.00489	13.6
2023	May 18 - June 25	38	0.00400	18.1
2024[a.c.]	May 23 - June 25	33	0.00497	15.5
All year's averages		**33.8**	**0.00540**	**16.7**

a. Start date within (+/- 1-2 days)
b. Significant decline in time series following initial date
c. Start date initial NDVI value below 0.4
d. 2001 MODIS Data gap

Table A2

Descriptive Statistics for all years from green-up to the end of caribou calving

Descriptive Statistics			
Year	**Mean NDVI**	**Median NDVI**	**Max NDVI**
2000	0.468	0.479	0.779
2001[a.c.d.]	0.404	0.418	0.629
2002	0.452	0.462	0.728
2003[a.c.]	0.458	0.469	0.762
2004[a.]	0.502	0.508	0.800
2005[a.c.]	0.458	0.469	0.784
2006[a.c.]	0.438	0.466	0.688
2007	0.478	0.494	0.806
2008	0.502	0.514	0.746
2009[b.]	0.446	0.464	0.759
2010[a.]	0.469	0.476	0.797
2011	0.470	0.479	0.773
2012	0.460	0.484	0.782
2013	0.478	0.495	0.731
2014[c.]	0.402	0.437	0.685
2015	0.499	0.513	0.759
2016[a.c.]	0.475	0.487	0.771
2017	0.464	0.474	0.779
2018[a.c.]	0.430	0.450	0.770
2019[a.c.]	0.488	0.504	0.801
2020[a.b.]	0.519	0.531	0.812
2021[a.]	0.456	0.472	0.746
2022[a.c.]	0.459	0.468	0.791
2023	0.445	0.464	0.670
2024[a.c.]	0.426	0.456	0.799
All year's averages	**0.462**	**0.477**	**0.758**

a. Start date within (+/- 1-2 days)
b. Significant decline in time series following initial date
c. Start date initial NDVI value below 0.4
d. 2001 MODIS Data gap

Table A3

Difference of initial and end of study period NDVI value, ΔNDVI *for first 10 days, and every year's midpoint day*

ΔNDVI			
Year	**NDVI Difference**	**First 10 days**	**Midpoint Day#**
2000	0.160	0.0063	10.5
2001[a.c.d.]	0.120	0.0063	9.5
2002	0.153	0.0025	18
2003[a.c.]	0.132	0.0070	11.5
2004[a.]	0.234	0.0027	17
2005[a.c.]	0.176	0.0058	18
2006[a.c.]	0.207	0.0082	15.5
2007	0.227	0.0020	17
2008	0.152	0.0015	11.5
2009[b.]	0.160	-0.0368**	19.5
2010[a.]	0.200	0.0016	18.5
2011	0.164	0.0051	16.5
2012	0.192	0.0043	18.5
2013	0.181	0.0013	18
2014[c.]	0.168	0.0020	19.5
2015	0.187	0.0027	19.5
2016[a.c.]	0.222	0.0054	21.5
2017	0.148	0.0023	17.5
2018[a.c.]	0.187	0.0054	20.5
2019[a.c.]	0.292	0.0074	22
2020[a.b.]	0.215	0.0062	17
2021[a.]	0.157	0.0028	16
2022[a.c.]	0.137	0.0051	14
2023	0.152	-0.0004**	19
2024[a.c.]	0.164	0.0033	16.5
All year's averages	**0.179**	**0.0024**	**16.9**

a. Start date within (+/- 1-2 days)
b. Significant decline in time series plot following initial date
c. Start date initial NDVI value below 0.4
d. 2001 MODIS Data gap

Table A4

ΔNDVI calculations for first half and second half of study period

ΔNDVI	First Half	Date Range		Second Half	Date Range	
Year	**ΔNDVI**	Start Date	End Date	**ΔNDVI**	Start Date	End Date
2000	0.00645	04-Jun-00	15-Jun-00	0.00890	15-Jun-00	25-Jun-00
2001[a.c.d.]	0.00630	31-May-01	10-Jun-01	0.00633	10-Jun-01	19-Jun-01
2002	0.00268	19-May-02	07-Jun-02	0.00567	07-Jun-02	25-Jun-02
2003[a.c.]	0.00617	02-Jun-03	14-Jun-03	0.00527	14-Jun-03	25-Jun-03
2004[a.]	0.00318	22-May-04	08-Jun-04	0.01060	08-Jun-04	25-Jun-04
2005[a.c.]	0.00478	20-May-05	07-Jun-05	0.00500	07-Jun-05	25-Jun-05
2006[a.c.]	0.00588	25-May-06	10-Jun-06	0.00753	10-Jun-06	25-Jun-06
2007	0.00459	22-May-07	08-Jun-07	0.00876	08-Jun-07	25-Jun-07
2008	0.00125	02-Jun-08	14-Jun-08	0.01245	14-Jun-08	25-Jun-08
2009[b.]	0.00330	17-May-09	06-Jun-09	0.00495	06-Jun-09	25-Jun-09
2010[a.]	0.00374	19-May-10	07-Jun-10	0.00717	07-Jun-10	25-Jun-10
2011	0.00394	23-May-11	09-Jun-11	0.00606	09-Jun-11	25-Jun-11
2012	0.00353	19-May-12	07-Jun-12	0.00694	07-Jun-12	25-Jun-12
2013	0.00183	20-May-13	07-Jun-13	0.00822	07-Jun-13	25-Jun-13
2014[c.]	0.00550	17-May-14	06-Jun-14	0.00305	06-Jun-14	25-Jun-14
2015	0.00195	17-May-15	06-Jun-15	0.00779	06-Jun-15	25-Jun-15
2016[a.c.]	0.00336	13-May-16	04-Jun-16	0.00705	04-Jun-16	25-Jun-16
2017	0.00194	21-May-17	08-Jun-17	0.00665	08-Jun-17	25-Jun-17
2018[a.c.]	0.00538	15-May-18	05-Jun-18	0.00370	05-Jun-18	25-Jun-18
2019[a.c.]	0.00636	12-May-19	03-Jun-19	0.00691	03-Jun-19	25-Jun-19
2020[a.b.]	0.00265	22-May-20	08-Jun-20	0.00735	08-Jun-20	25-Jun-20
2021[a.]	0.00344	24-May-21	09-Jun-21	0.00638	09-Jun-21	25-Jun-21
2022[a.c.]	0.00421	28-May-22	11-Jun-22	0.00557	11-Jun-22	25-Jun-22
2023	0.00100	18-May-23	06-Jun-23	0.00700	06-Jun-23	25-Jun-23
2024[a.c.]	0.00388	23-May-24	09-Jun-24	0.00613	09-Jun-24	25-Jun-24
All year's averages	**0.00389**	**21-May-12**	**07-Jun-12**	**0.00686**	**07-Jun-12**	**24-Jun-12**

a. Start date within (+/- 1-2 days)
b. Significant decline in time series following initial date
c. Start date initial NDVI value below 0.4
d. 2001 MODIS Data gap

Appendix B: *Modis Time Series Maps*

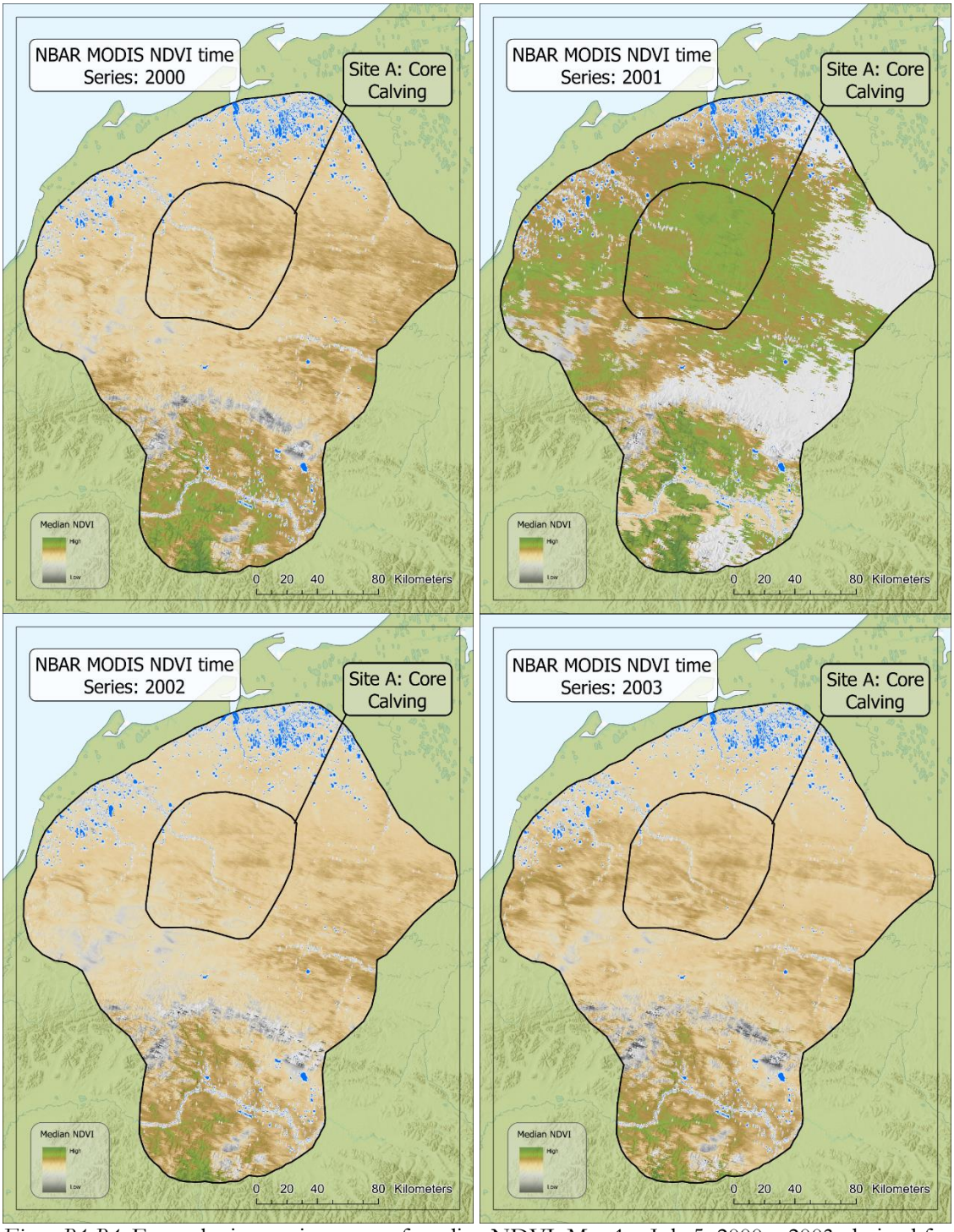

Figure B1-B4: Example time series maps of median NDVI, May 1 – July 5, 2000 – 2003, derived from the NBAR MODIS dataset.

Appendix C: *HLS Timeseries Maps*

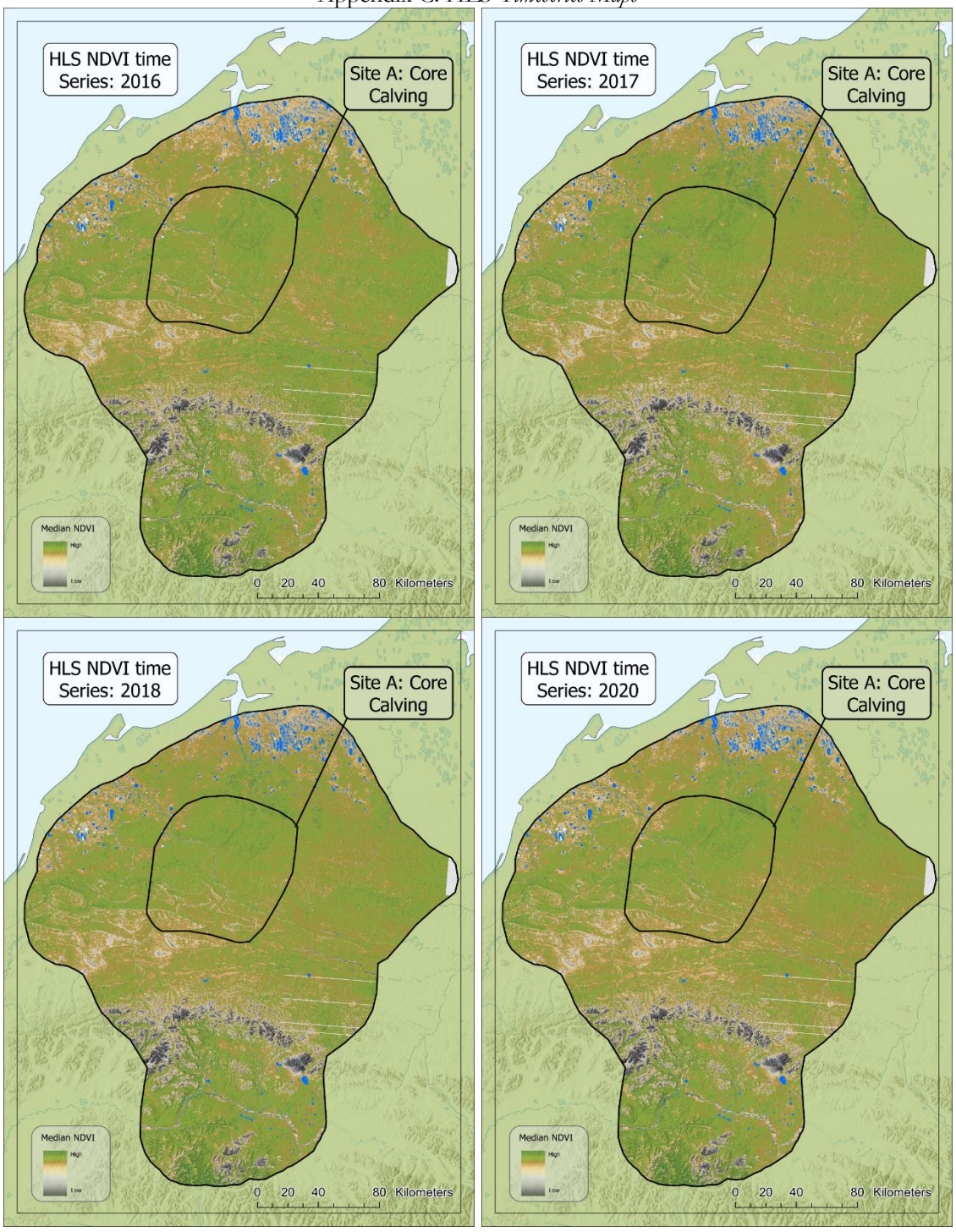

Figure C1-C4: Example time series maps of median peak NDVI, 2016 – 2020, derived from the HLS dataset.

Appendix D: NDVI Time Series Plots

Figure D1-D8: Example of time series plots depicting median and maximum NDVI from the NBAR MODIS dataset, May 1 – July 5, 2000 – 2007.